

3D PARALLEL SIMULATION MODEL OF CONTINUOUS BEAM ELECTRON CLOUD INTERACTIONS

A.Z. Ghalam, T. Katsouleas, University of Southern California, Los Angeles, California, USA

V.K. Decyk, C.K. Huang, W.B. Mori, University of California at Los Angeles, Los Angeles,
California, USA

G. Rumolo, GSI, Darmstadt, Germany

E. Benedetto, F. Zimmermann, CERN, Geneva, Switzerland

Abstract

Long-term beam-electron cloud interaction is modeled with a 3D parallel continuous model originally developed for plasma wakefield acceleration modeling. The simulation results are compared with the two macro-particle model for strong head-tail instability. The two macro-particle model qualitatively captures some of the instability features of the beam. The code is then used to model and make predictions for the beam dynamics in the presence of an electron cloud for several present and future circular machines around the world.

INTRODUCTION

Due to the importance of the electron cloud problem in many existing and planned circular machines around the world[1-9], many simulation codes have been developed to model the dynamics of the beam in the electron cloud. Most of these simulation codes such as HEAD-TAIL developed at CERN [10] are based on the single kick approximation where the cloud is lumped at discrete locations along the ring. While this approximation is very efficient as far as the computational costs are concerned, it has serious limitations [11]. The second simulation model recently developed at USC/UCLA is based on Particle-In-Cell method originally in use for plasma wakefields [12]. In this model the cloud is spread all over the ring and the beam continuously interacts with the electron cloud [12-15].

In this paper, QuickPIC as a more realistic model is used to model long-term beam- electron cloud interaction. This paper is organized as follows. In the second section some of the instability features of the beam are described with the two macro-particle model for strong head-tail instability. The last section is dedicated to the specific QuickPIC simulation results for SLAC-PEP-II and CERN-LHC storage ring.

COMPARING THE SIMULATION RESULTS WITH THE TWO MACRO- PARTICLE MODEL

In this section, some of the instability features of beam-electron cloud interaction observed in QuickPIC simulations are explained by the two macro-particle model for strong head-tail instability.

First, the validity of the instability criterion obtained in the two macro-particle modeling is investigated with QuickPIC simulations.

During the first half of the synchrotron period, $0 < s/c < T_s/2$, the equations of motion for the two macro-particles are:

$$\begin{aligned} y_1'' + \left(\frac{\omega_\beta}{c}\right)^2 y_1 &= 0 \\ y_2'' + \left(\frac{\omega_\beta}{c}\right)^2 y_2 &= ky_1 \end{aligned} \tag{1}$$

where ω_β is the betatron frequency of the particles in the transverse plane and k is the coupling term between the two particles. In this case k is proportional to transverse electron cloud wake produced at particle 2 caused by particle 1. Similarly, during the second half period, the same equations apply with indices 1 and 2 exchanged. The right-hand side of the harmonic oscillator equation for the tail particle (index 2) corresponds to the force from the electron cloud wakefields generated due to the beam-electron cloud interaction. In writing these equations, only the first order wake function is considered for simplicity [11].

The stability condition for the center of charge motion dictates the following condition on the instability parameter, G :

$$G = \frac{k\pi c^2}{2\omega_\beta\omega_s} < 2 \tag{2}$$

The instability parameter, G depends on several parameters as shown in Eq.(2). In this section, the validity of the above criterion for beam stability in the presence of the electron cloud is investigated.

For the purpose of demonstration, the CERN-SPS parameters have been used in these simulations. These parameters are summarized in Table 1 of Appendix-A.

First Eq.(2) is used to find the instability threshold for the electron cloud density. The instability parameter G , can be specified once k is determined. This coefficient can be found by QuickPIC simulations. To find the wake force at the tail, a point charge is set at the head of the

bunch and the wake force is obtained at the location of the tail. Then the point charge is moved transversely and the wake force is again obtained at the tail. Repeating this process for different transverse offsets of the head, a plot of normalized wake force ($\frac{F_{\perp}}{\gamma mc^2}$) versus transverse offset of the tail can be found as shown in Fig. 1.

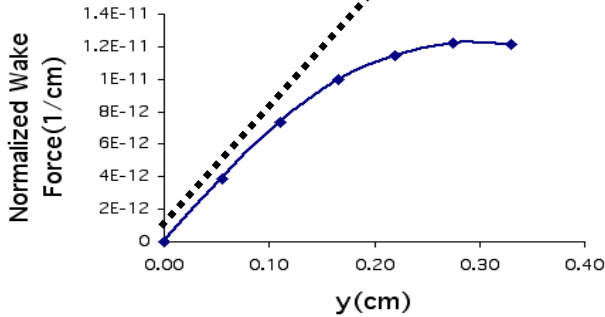


Figure 1: Normalized Wake force ($\frac{F_{\perp}}{\gamma mc^2}$) at the tail of the bunch versus head offset in vertical plane

The rms spot size of the bunch for CERN-SPS is 0.2cm and as can be seen from the plot, it lies in the non-linear region of the wakefield. The linearized wake force is shown as a dotted line the slope of which is k in Eq. (2). It is worth mentioning that the linearized wake force obtained here matches surprisingly well with an approximate expression for the normalized wake force [17]:

$$\frac{F_{\perp}}{\gamma mc^2} = \frac{4\pi r_0 \rho}{\gamma} y \quad (3)$$

where r_0 is the classical radius of a proton, ρ is the electron cloud density and γ is the relativistic factor.

To examine the instability criterion in Eq. (2), we have to find a value of k (or in other words a cloud density) for which the instability parameter, G , approaches 2. Based on Eq. (2), the head-tail instability occurs at a cloud density of $2 \times 10^6/\text{cm}^3$. Next, the threshold for instability is obtained by direct QuickPIC simulations. Based on QuickPIC simulations, the centroid motion starts growing exponentially at electron cloud densities around $10^7/\text{cm}^3$. Thus, the instability criterion based on macro-particle modeling underestimated the threshold of instability.

RESULTS FOR SPECIFIC CURRENT AND FUTURE MACHINES

In this section, QuickPIC simulation results for SLAC-PEP-II storage ring and the CERN-LHC ring are given. The spot size growth of the beam is predicted and the instability threshold for electron cloud density is estimated.

a) SLAC-PEP-II Lower Energy Ring (LER) Storage Ring

The parameters used for PEP-II LER simulations are summarized in Table 2 in Appendix-A. As seen by the table, the box size dimension is $2\text{cm} \times 1\text{cm}$ however the PEP-II LER has a round cross section 4.5cm of radius. The actual dimension of the pipe is much larger than the beam dimensions. Modeling the system with the actual pipe dimensions requires having many grids in the transverse plane in order to resolve the beam dimensions and this slows the simulation run time and makes it impractical to model long-term beam dynamics.

Since the pipe size is much larger than the beam spot size, the boundary conditions may be inconsequential to the long-term beam and electron cloud dynamics. To reduce the computational costs, the simulation box is reduced to the sizes indicated in Table 2. QuickPIC simulations confirms that the transverse wakefield in the reduced box size case differ from the original wakefields by less than 10%.

Next, the long-term beam dynamics and instabilities have been analyzed for this ring. Figure 2 shows the horizontal spot size growth of the beam over 1000 turns of beam evolution around the ring for different electron cloud densities. As can be seen from the figure there is no growth for cloud densities of $5 \times 10^5/\text{cm}^3$ and $10^6/\text{cm}^3$. For density of $10^7/\text{cm}^3$, the horizontal spot size grows steadily. Based on this simulation the cloud density threshold for horizontal beam blow-up is around $5 \times 10^6/\text{cm}^3$.

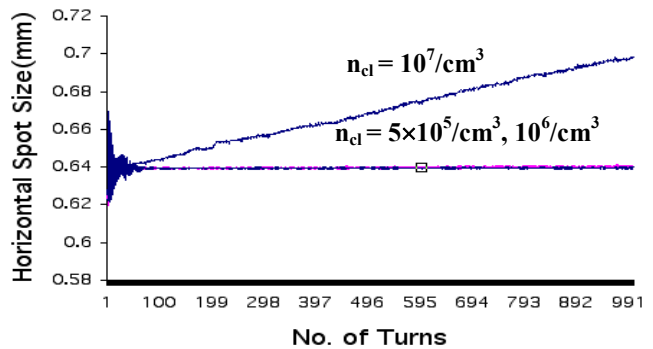


Figure 2: Horizontal spot size growth of the beam at PEP-II LER ring for different cloud densities

Since the beam at PEP-II LER ring is flat, the dynamics of the beam in the vertical plane is expected to be different than that of the horizontal plane as illustrated in Figure 3. This figure shows the vertical spot size growth with different densities.

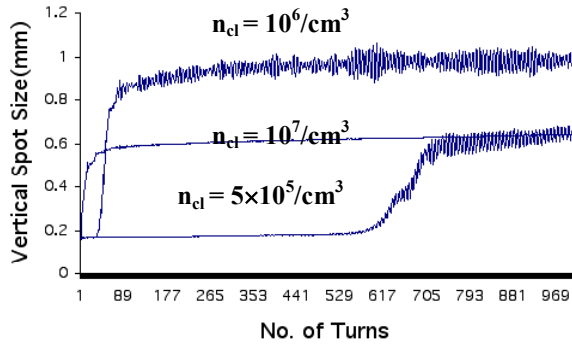


Figure 3: Vertical spot size of the beam at PEP-II LER with different cloud densities

For the cloud density of $10^7/\text{cm}^3$, the spot size grows drastically in the first 100 turns and then the growth rate becomes much smaller. For the cloud densities of 10^6 and $5 \times 10^5/\text{cm}^3$, the situation is the opposite. There is almost no growth observed in the first turns and then the growth is drastic. While there is a consistent trend toward earlier growth the higher the cloud density, the saturated spot size does not appear to increase monotonically with cloud density. At this point we have no complete explanation for this non-monotonic behavior.

b) CERN-LHC

Next, the dynamics of the beam in the LHC ring is investigated with the QuickPIC simulations. The parameters for the simulation can be found in Table 3 in Appendix-A.

A typical Electron cloud density in this collider is predicted to be $6 \times 10^5 \text{cm}^{-3}$ [16] and electron cloud would cause head-tail type instability in horizontal and vertical planes.

The spot size growth is investigated with QuickPIC simulations. Figure 4 shows the horizontal and vertical spot size growth for 2000 turns of beam evolution over the ring.

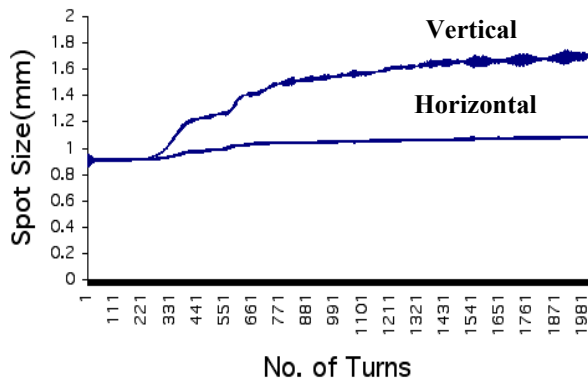


Figure 4: Horizontal and vertical spot size growth at CERN-LHC in a field free region.

APPENDIX-A: TABLE OF PARAMETERS FOR DIFFERENT MACHINES

Table 1: CERN-SPS parameters used in the simulations

RMS Horizontal Spot Size (mm)	2
RMS Vertical Spot Size (mm)	2
RMS Bunch Length (cm)	30
Horizontal Box Size (mm)	80
Vertical Box Size (mm)	40
Bunch Population	10^{11}
Horizontal Emittance (μm)	0.1
Vertical Emittance (μm)	0.1
Momentum Spread	2.48E-3
Beam Momentum (GeV/c)	26
Circumference (km)	6.9
Horizontal Betatron Tune	26.22
Vertical Betatron Tune	26.18
Synchrotron Tune	0.005
Electron Cloud Density (cm^{-3})	$10^6 - 10^7$
Number of Grids	128x64x64
Number of Beam Particles	1048576
Number of Electron cloud Particles	16384

Table 2: SLAC-PEP-II Parameters used for the simulations

RMS Horizontal Spot Size (mm)	0.623
RMS Vertical Spot Size (mm)	0.164
RMS Bunch Length (cm)	1.3
Horizontal Box Size (mm)	20
Vertical Box Size (mm)	10
Bunch Population	10^{11}
Horizontal Emittance (μm)	141
Vertical Emittance (μm)	8.806
Momentum Spread	7.7×10^{-4}
Beam Momentum (GeV/c)	3.19
Circumference (m)	2200
Horizontal Betatron Tune	21.649
Vertical Betatron Tune	19.564
Synchrotron Tune	0.025
Electron Cloud Density (cm^{-3})	2×10^5
Number of Grids	256x128x64
Number of Beam Particles	1048576
Number of Electron cloud Particles	36864

Table 3: CERN-LHC parameters used in the simulations

RMS Horizontal Spot Size (mm)	0.884
RMS Vertical Spot Size (mm)	0.884
RMS Bunch Length (cm)	11.5
Horizontal Box Size (mm)	18
Vertical Box Size (mm)	18
Bunch Population	1.1×10^{11}
Average Horizontal Beta Function	66
Average Vertical Beta Function	77.5
Momentum Spread	4.68×10^{-4}
Beam Momentum (GeV/c)	450
Circumference (km)	6.9
Horizontal Betatron Tune	64.28
Vertical Betatron Tune	59.31
Synchrotron Tune	0.0059
Electron Cloud Density (cm ⁻³)	6×10^5
Number of Grids	64×64×64
Number of Beam Particles	524288
Number of Electron cloud Particles	16384

REFERENCES

- [1] H. Fukuma, K. Cornelis, F.-J. Decker, R. Macek, E. Metral, W. Fischer in *Proceedings of ELOUD'02*, CERN, Geneva 15-18 April 2002, edited by G. Rumolo and F. Zimmermann, Yellow Report CERN-2002-001
- [2] G. Rumolo, F. Ruggiero and F. Zimmermann, Phys. Rev. ST Accel. Beams, 4, 012801 (2001).
- [3] M. Jimenez *et al.*, in *Proceedings of ELOUD'02*, CERN, Geneva 15-18 April 2002, edited by G. Rumolo and F. Zimmermann, Yellow Report CERN-2002-001
- [4] A. Rossi, G. Rumolo, and F. Zimmermann, in *Proceedings of ELOUD'02*, CERN, Geneva 15-18 April 2002, edited by G. Rumolo and F. Zimmermann, Yellow Report CERN-2002-001
- [5] G. Arduini, K. Cornelis, W. Hoefle, G. Rumolo, and F. Zimmermann, in *Proceedings of PAC2001*, Chicago (2001)
- [6] K. Oide, "Observation and Cure of the Electron Cloud Effect at the KEKB Low Energy Ring", Chamonix XI, CERN SL-2001-003 (DI)
- [7] S. S. Win *et al.*, "Observation of Transverse Coupled Bunch Instability at KEKB", in *Proceedings of APAC2001*, Beijing (2001)
- [8] R. Cappi, M. Giovannozzi, E. Metral, G. Rumolo, and F. Zimmermann, Phys. Rev. ST Accel. Beams 5, 094401 (2002)
- [9] K. Ohmi, "Particle in Cell Simulations of Beam-Electron Cloud Interactions", PAC2001 Chicago.
- [10] G. Rumolo *et al.*, 'Electron Cloud Simulations: Beam Instabilities and Wakefields', in *Proceedings of ELOUD'02*, CERN, Geneva, 2002.
- [11] A. Chao 'Physics of Collective Beam Instabilities in High Energy Accelerators' Wiley & Sons 1993.
- [12] A. Ghalam *et. al.*, '3-D Parallel Simulation of Continuous Beam-Cloud Interactions', to be appeared in *Proceedings of ELOUD'04*, Napa Valley, California
- [13] E. Benedetto *et. al.*, 'Simulation of Transverse Single Bunch Instabilities and Emittance Growth caused by Electron Cloud in LHC and SPS', to be appeared in *Proceedings of ELOUD'04*, Napa Valley, California
- [14] C. Hunag *et. al.*, in proceedings of the 18th Annual Review of Progress in Applied Electromagnetics, Monterey, CA, 2002, p.557
- [15] G. Rumolo, A. Z. Ghalam *et. al.*, Phys. Rev. ST Accel. Beams, Vol. 6, 081002, 2003.
- [16] O. Bruning *et al.* (eds.), LHC Design Report Vol. 1: The LHC Main Ring, CERN-2004-003 (2004)
- [17] K. Ohmi *et. al.*, 'Head-Tail Instability Caused by Electron Clouds in Positron Storage Rings', PRL, Vol. 85, No. 18, 2000.